

Ling Liu · Yaomin Zhao · Qin Zhou · Hong Xu
Chongjun Zhao · Zhiyu Jiang

Nano-polypyrrole supercapacitor arrays prepared by layer-by-layer assembling method in anodic aluminum oxide templates

Received: 28 June 2005 / Revised: 13 July 2005 / Accepted: 4 August 2005 / Published online: 24 September 2005
© Springer-Verlag 2005

Abstract A novel method for preparing nano-supercapacitor arrays, in which each nano-supercapacitor consisted of electropolymerized Polypyrrole (PPy) electrode / porous TiO₂ separator / chemical polymerized PPy electrode, was developed in this paper. The nano-supercapacitors were fabricated in the nano array pores of anodic aluminum oxide template using the bottom-up, layer-by-layer synthetic method. The nano-supercapacitor diameter was 80 nm, and length 500 nm. Based on the charge/discharge behavior of nano-supercapacitor arrays, it was found that the PPy/TiO₂/PPy array supercapacitor devices performed typical electrochemical supercapacitor behavior. The method introduced here may find application in manufacturing nano-sized electrochemical power storage devices in the future for their use in the area of microelectronic devices and microelectromechanical systems.

Keywords Nano-supercapacitor arrays · Polypyrrole · Anodic aluminum oxide template · Bottom-up, layer-by-layer synthetic method

Introduction

Polypyrrole (PPy) is one of the important conducting polymers due to its electrochemical reversibility, relative environmental stability, and the ease of preparation

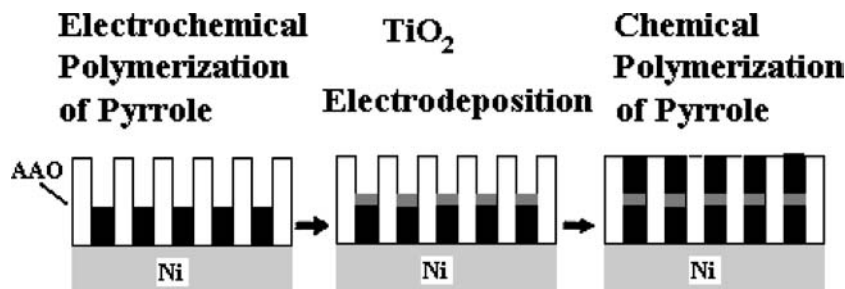
through chemical or electrochemical routes [1–5]. Based on its reversible electrochemical redox reaction behavior it has been investigated as the electrode material for rechargeable batteries [6, 7]. Recently many papers reported that polypyrrole can be used as the electrode material for supercapacitors [8–14]. Ingram and co-workers [13–15] suggested that during the oxidation process polypyrrole becomes p-doped material and one additional electron can be removed for every third monomer unit in the chain. Seven electrons were removed for every three monomer units, and the residual positive charge on the polymer is balanced by the negative charges of dopant anions. The large capacitive response of the PPy electrode is mainly due to this faradaic process in the potential region lower than 0.3 V. The capacitance of the electrode also partly comes from the charge/discharge process of the double layer in the potential region higher than 0.3 V, where the anodic current curves are paralleled approximately with the cathodic current curves with relative high current margins [13]. In fact, the apparent capacitance of PPy electrode consists of redox capacitance and double-layer capacitance. It was found that the capacitive behavior of the PPy electrode only appears when the electrode was very thin (ca. 1 μm in thick) [15].

Nowadays, the design of nano-devices is an intensive research field, owing to the growing miniaturization of microelectronic devices and microelectromechanical systems (MEMS). Various methods have been used to fabricate ultra-thin microelectrochemical power sources, such as pulse laser deposition [16], photolithography techniques [17], radio-frequency magnetron sputtering [18], and a computer inkjet printing method introduced in our previous paper [19]. However, to our knowledge, quasi-one-dimensional nano-sized battery or supercapacitor has not been explored. The methods for preparing one-component nano-material are now very common. There are also some examples for synthesizing multi-component nano-materials. The anodic aluminum oxide (AAO) membrane with ordered straight nano-channels is

L. Liu · Y. Zhao · Q. Zhou · H. Xu · Z. Jiang (✉)
Department of Chemistry and Shanghai Key Laboratory
of Molecular Catalysis and Innovative Materials,
Fudan University, Shanghai 200433, China
E-mail: zyjiang@fudan.ac.cn
Tel.: +86-21-65642404
Fax: +86-21-65641740

C. Zhao
Photon Craft Project, Shanghai Institute of Optics & Fine
Mechanics, Chinese Academy of Sciences and Japan
Science and Technology Agency, Shanghai 201800, China

Scheme 1 Schematic diagram of the process for the fabrication of the PPy nano-fiber array supercapacitors



well known as the template for fabricating the nano-array materials such as metal, inorganic composite, conducting polymer fibers or tubes, and multi-metal striped rods [20–25]. The diameter and depth of pores in the AAO membrane can be adjusted by controlling the anodizing voltage, temperature, the selection of electrolytes such as oxalic, sulfuric, and phosphoric acid solutions, and the anodizing time [26, 27]. Herein, we first introduce the preparation of nano-supercapacitor arrays within the pores of AAO templates. The nano-supercapacitors were fabricated using layer-by-layer, from bottom to top assembling technique. This method may benefit the development of nano-electronics.

Experimental

Pyrrole (from Aldrich) was distilled prior and stored at 5°C under nitrogen in the absence of light. All solutions were prepared from analytical grade chemicals and highly purified water.

Preparation of AAO templates

The AAO templates were prepared from aluminum sheet using a two-step anodizing method in oxalic acid solution according to the procedure introduced in Refs. [26, 27]. High-purity aluminum sheet (99.99%) was degreased, electropolished in a mixture solution of EtOH and HClO₄ (4:1 in v/v), anodized at 40 V in 0.5 M H₂C₂O₄ solution for 1 h and then moved into 0.4 M H₃PO₄ + 0.2 M H₂C₁O₄ solution at 60°C to dissolve the oxide membrane. After this removal, the Al plate was anodized again for 2–4 h. Then the background Al layer was removed from the AAO membrane via a replacement reaction by immersing the sample in a saturated HgCl₂ solution. The AAO membrane was put into 20 wt% sulfuric acid solution until the barrier layer at the bottom of AAO membrane was dissolved completely. Through washing and drying, the AAO membrane with open nano-pore arrays was obtained.

Preparation of PPy nano-fiber array electrode

Electrochemical polymerization of pyrrole was carried out in a conventional three-compartment cell in deoxy-

genated solution containing 0.1 M pyrrole monomer and 0.2 M LiClO₄. A nickel-coated AAO electrode prepared by sputtering Ni on one side of the AAO membrane was used as the working electrode. A Pt foil and an Ag/AgCl electrode were used as counter electrode and reference electrode, respectively. The PPy nano-fibers were potentiostatically polymerized in the pores of the AAO membrane at a potential of 0.8 V (vs. Ag/AgCl). It has been assumed that the positive charge of 240 mC/cm² corresponds to a PPy layer with the thickness of 1 μm for depositing on a smooth flat electrode [28]. The length of deposited PPy fiber in the AAO pore can be controlled coulometrically by considering the diameter, depth of pores and the volume density of pores in the AAO membrane. The electrodes were rinsed carefully with a large amount of double-distilled water, and dried at room temperature. Then the PPy nano-fiber array electrodes were obtained.

Preparation of nano-fiber supercapacitor arrays

The PPy/TiO₂/PPy nano-supercapacitor in the nanopore of the AAO template was structured in a sandwich form via bottom-up, layer-by-layer synthetic procedure, as shown in Scheme 1. It consisted of three parts: electrochemically polymerized PPy electrode/porous TiO₂ separator/chemically polymerized PPy electrode.

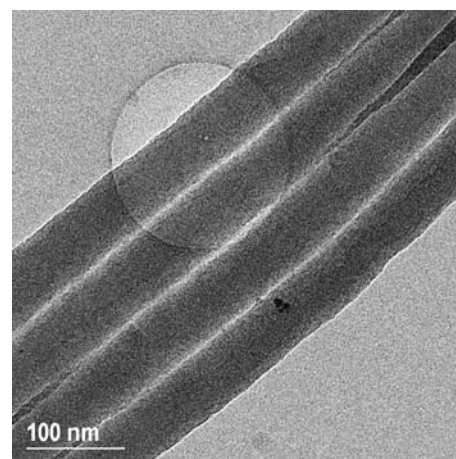
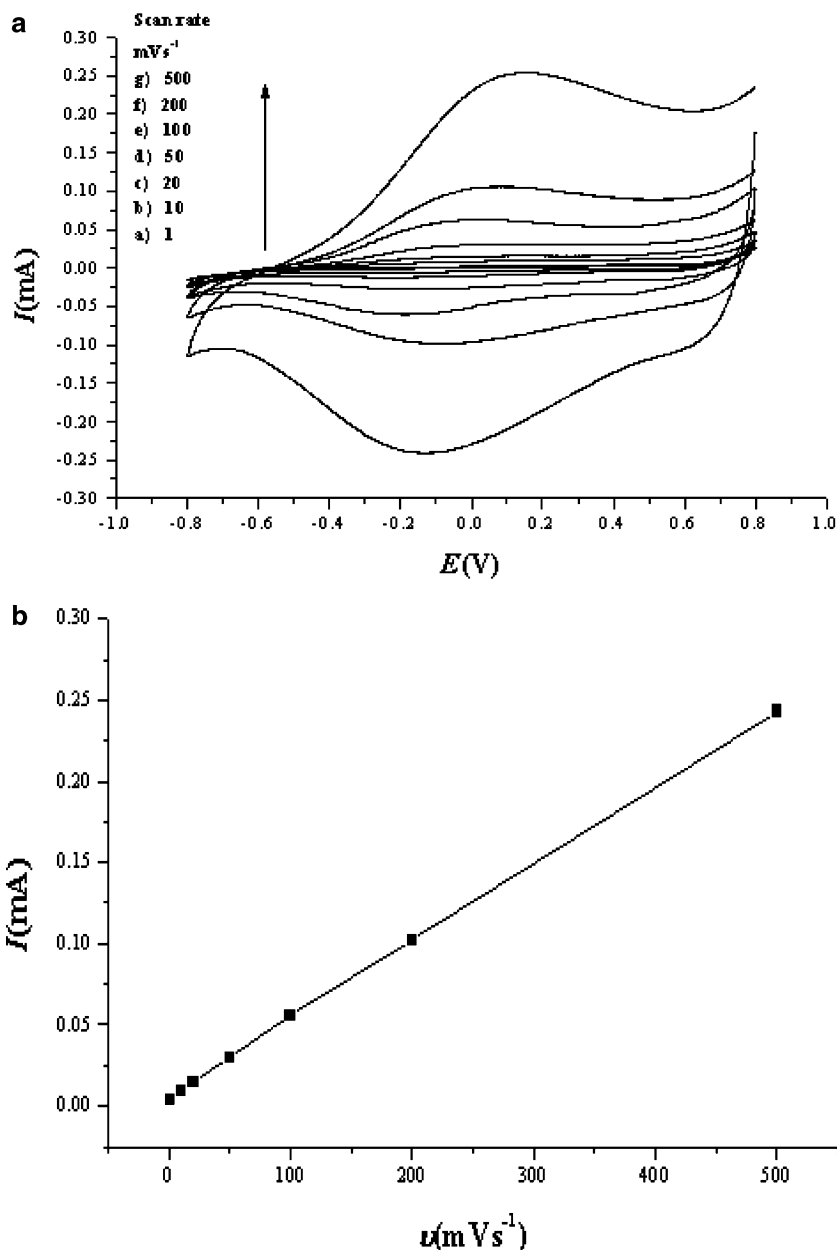


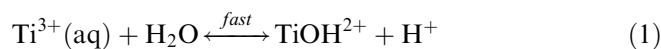
Fig. 1 TEM image of PPy nano-fibers after removal of the alumina matrices of the AAO membrane

Fig. 2 **a** Cyclic voltammograms of PPy nano-fiber array electrode in 0.2 M LiClO₄ solution at different potential scan rates. **b** Cathodic peak currents as a function of potential sweep rate. Surface area 1 mm², length of fiber 500 nm



- (1) First, PPy was electrochemically deposited in the pores using the procedure introduced previously. The length of PPy fibers in the pores was controlled coulometrically to be approximately one-third of the depth of the nano-pores.
- (2) The PPy nano-fiber AAO array film obtained from the first step was moved to another cell for separator preparation. Because PPy is a conducting material, especially when it is in anion-doped state in the higher potential region of 0.4–0.8 V, the separator material, TiO₂ nano-particles could be electrochemically deposited on the top of short PPy nano-fibers in the pores via an anodic oxidation reaction of TiCl₃ followed by a heat treatment. The procedure was similar to that of preparing normal TiO₂ films described in Ref. [29]. TiO₂ nano-particles were electrodeposited from a solution saturated with

nitrogen of 1.5% TiCl₃, 0.016% carboxymethyl-cellulose (CMC), 1 M Na₂CO₃ buffered to pH 2.2 at a potential of 0.1 V (saturated calomel electrode (SCE)) for 2 min. The reaction processes are as follows [29]:



The samples were then washed with 0.01 M HCl, water, and ethanol. After drying under the irradiation of an infrared lamp at about 90°C for 1 h, TiO₂ nano-particles were formed as the material of the separator located on top of the short PPy fibers in the nano-pores of the AAO template.

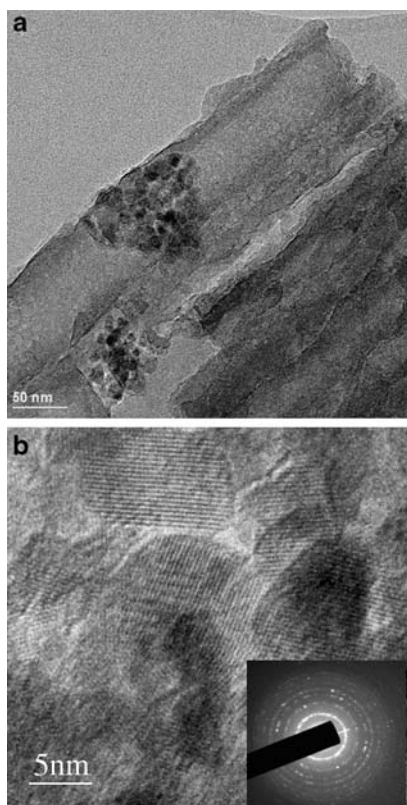
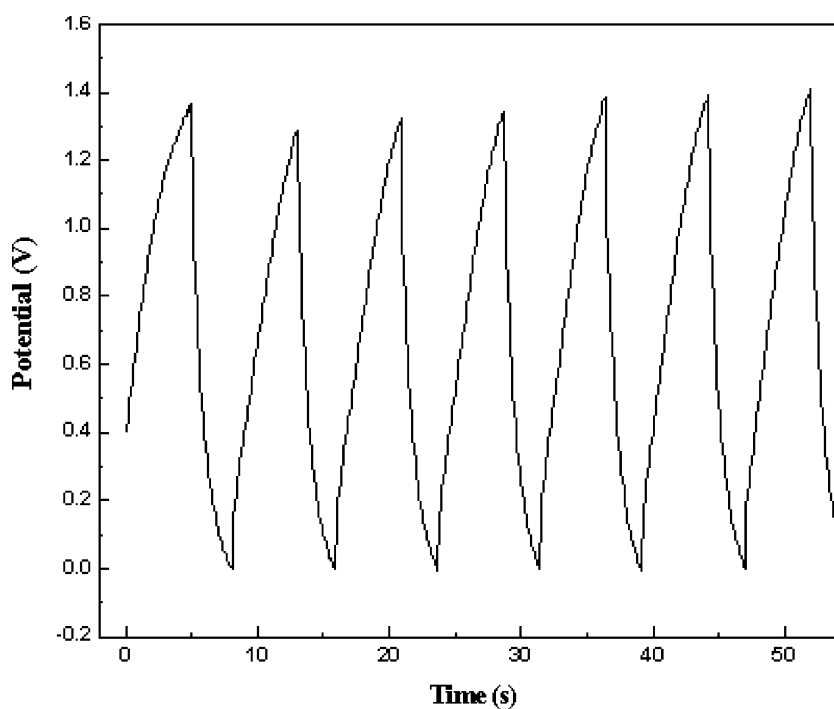


Fig. 3 TEM images of PPy/TiO₂/PPy nano-supercapacitor (a) and nano TiO₂ particles (b)

- (3) Finally, another terminal PPy electrode was prepared above the nano TiO₂ separator layer within the pores of the AAO template using a chemical oxidation method, in which ammonium persulfate was used as

Fig. 4 Cyclic charge–discharge curves of PPy/TiO₂/PPy nano-capacitors, both charge and discharge currents and times were 1 nA and 5 s



the oxidation agent [30]. The dry Ni/PPy/TiO₂ AAO membrane was immersed in 2.2 M ammonium persulfate solution for 30 min. The ammonium persulfate solution could enter into the nano-pores due to capillary effect. After drying, it was dipped into 0.1 M pyrrole + 0.2 M LiClO₄ solution and kept 6–10 h for complete polymerization. Then the process was repeated once. After washing, drying, and then adding a small drop of 0.2 M LiClO₄ solution as the electrolyte of the supercapacitor, the PPy/TiO₂/PPy nano-fiber array supercapacitor was obtained.

Morphology and electrochemical measurements

The morphologies of the AAO membrane, PPy nano-fibers, TiO₂ nano-particles, and nano PPy/TiO₂/PPy supercapacitor were examined by a Philip XL30 scanning electron microscopy (SEM) and a JEOL JEM 2011 high-resolution transmission electron microscopy (TEM). For the observation of nano-supercapacitor microstructure, the PPy/TiO₂/PPy nano-fiber array membrane was ground slightly in absolute alcohol. A drop of the solution was added onto the carbon-coated copper grid. Then the dried grid was used for TEM measurement.

The electrochemical properties of the PPy array electrodes were measured in a three-chamber cell with Pt counter electrode and Ag/AgCl reference electrode in 0.2 M LiClO₄ aqueous solution. The cyclic voltammety curves of the PPy array electrodes were obtained using CHI660 electrochemical station. The charge–discharge properties of the nano-fiber array supercapacitors were investigated using CHI660 electrochemical station.

Results and discussion

The SEM image of the AAO template shows a densely packed hexagonal array of uniform pores with diameters of 80 nm (not shown here). The volume density of the pores was estimated to be about 50% according to the pore number and pore diameter per unit area. Figure 1 shows the TEM image of the PPy nano-fibers obtained after the removal of the alumina matrix in 6 M NaOH solution. It can be seen that the diameter of the PPy nano-fibers is 80 nm, which is similar to the pore diameter in the AAO membrane.

Figure 2a shows the cyclic voltammograms of a Ni/PPy nano-fiber array electrode in 0.2 M LiClO₄ solution at different potential sweep rates. A pair of redox current peaks appears at potentials of +0.05 and -0.09 V vs. Ag/AgCl, respectively, for each curve. They correspond to the doping and dedoping processes of ClO₄⁻ ions in PPy, respectively [31]. The reaction could have taken place both on the top and round the sides of each nano PPy fiber, because the electrolyte could permeate into the pores of the AAO film. Figure 2b shows the linear relationship between cathodic peak current and the potential sweep rate, which reflects the electrochemical characteristics of the thin film electrode [32]. When the sweep rate is less than 500 mV/s, in the potential region higher than 0.3 V the anodic current curves are paralleled approximately with the cathodic current curves with relative high current margins. The behavior reflects the characteristic of charge/discharge of the double layer. According to the equation $C = \Delta I / 2v$, the double layer capacity of an electrode can be calculated, where ΔI is the margin between paralleled anodic and cathodic current curves, and v the potential sweep rate. The double layer capacity of the PPy nano-fiber array electrode was calculated to be 44 mF per apparent cm², which may be ascribed to the ordered structure with enhanced interfacial area. The specific surface area of the PPy nanofiber is very high due to its diameter, which is as small as 80 nm, and high aspect ratio. Therefore the combination of the double layer capacity in the high-potential region with the capacity from the faradaic process in the low-potential region makes it possible that the PPy nano-fiber electrodes can be used as the electrodes for nano-supercapacitors.

The TEM image shows that the PPy/TiO₂/PPy nano-fiber array supercapacitors were about 80 nm in diameter within the nano-pores of the AAO template (Fig. 3a). The electropolymerized PPy is located at the down side of the pore, while chemically polymerized PPy upside. The layer between them is the separator, which consists of many loosely aggregated TiO₂ nano-particles. The high-resolution transmission electron microscopy (HRTEM) and selected-area electron diffraction (SAED) images (measured by JEOL JEM 2011 transmission electron microscopy) (Fig. 3b) shows that the TiO₂ particles with diameters of about 10–15 nm are well crystallized. It should be mentioned that during the

electrochemical synthesis of TiO₂ it was necessary to add a small amount of CMC into the electrolyte in order to produce a loose TiO₂ precipitation layer. Otherwise the TiO₂ layer would be very dense which causes the high resistance and low discharge ability of the nano-supercapacitors. The loose aggregation structure benefits the transfer of ions through the separator, and therefore can reduce the internal resistance of the PPy/TiO₂/PPy nano-supercapacitors.

The procedure for measuring the charge–discharge curves of the PPy/TiO₂/PPy nano-fiber array supercapacitors was as follows. An external power source (from CHI660 electrochemical workstation) was connected with a PPy/TiO₂/PPy nano-fiber array supercapacitor device. The positive terminal of the external power source was connected to the Ni side of the nano-fiber array supercapacitor device. The negative terminal was connected to the chemically polymerized PPy electrode of the nano-fiber array supercapacitor device using a thin tungsten wire with a diameter of about 1 μm. Figure 4 presents the charge–discharge curves of the PPy/TiO₂/PPy nano-fiber array supercapacitor device under constant charge or discharge current 1 nA, in the voltage range of 0–1.4 V. Both charge and discharge times are 5 s. The charge and discharge curves are roughly linear. It exhibits the characteristics of the supercapacitor with cyclic ability. The capacitance of the nano-fiber array supercapacitor can be calculated by the equation of $C = It / \Delta V$, where I is the current, t the time and ΔV voltage difference. The capacitance was calculated as 3.5 nF. This capacitance may be attributed to the many PPy/TiO₂/PPy nano-fiber supercapacitors in array, in contact with tungsten wire.

Conclusion

In summary, the results demonstrate that nano-supercapacitors can be assembled within the nano-pores in an AAO template using bottom-up, layer-by-layer synthetic technique. The advantage of this method is very simple for fabricating nano sized electrochemical power sources. The PPy/TiO₂/PPy nano-supercapacitor performs in a behavior typical of the electrochemical supercapacitor. Such multi-component structures can be tailored through the selection of the composition in the context of an integrated microelectrode device. The method introduced here may find application in developing microelectronic devices and MEMS.

Acknowledgements The work was supported by the National Science Foundation of China, Fudan University Graduate Innovative Foundation and Shanghai Nanotechnology Promotion Center (Project No. 0259 nm 023).

References

1. Lonergan MC (1997) *Science* 278:2103
2. Kaneto K, Takeda S, Yoshino K (1985) *Jpn J Appl Phys* 24:L553

3. Gao J, Heeger AJ, Lee JY, Kim CY (1996) *Synth Met* 82:221
4. Lu W, Fadeev AG, Qi B, Smela E, Mattes BR, Ding J, Spinks GM, Mazurkiewicz J, Zhou D, Wallace GG, MacFarlane DR, Forsyth SA, Forsyth M (2002) *Science* 297:983
5. Xie H, Yan M, Jiang Z (1997) *Electrochim Acta* 42:2361
6. Panero S, Prospero P, Scrosati B (1987) *Electrochim Acta* 32:1465
7. Novak P, Vielstich W (1990) *J Electrochem Soc* 137:1036
8. Jurewicz K, Delpeux S, Bertagna V, Beguin F, Frackowiak E (2001) *Chem Phys Lett* 347:36
9. Hashmi SA, Upadhyaya HM (2002) *Solid State Ionics* 152–153:883
10. Zhang Q, Zhou X, Yang H (2004) *J Power Sources* 125:141
11. Sung J-H, Kim S-J, Lee K-H (2004) *J Power Sources* 133:312
12. Noh KA, Kim D-W, Jin C-S, Shin K-H, Kim JH, Ko JM (2004) *J Power Sources* 124:593
13. Ingram MD, Staesche H, Ryder KS (2004) *J Power Sources* 129:107
14. Ingram MD, Staesche H, Ryder KS (2004) *Solid State Ionics* 169:51
15. Ingram MD, Pappin AJ, Delalande F, Poupard D, Terzouli G (1998) *Electrochim Acta* 48:1601
16. Striebel KA, Deng CZ, Wen SJ, Cairns EJ (1996) *J Electrochem Soc* 143:1821
17. Sung J-H, Kim S-J, Lee K-H (2003) *J Power Sources* 124:343
18. Miura T, Kishi T (1995) *Mat Res Soc Symp Proc* 393:69
19. Xu F, Wang T, Li W, Jiang Z (2003) *Chem Phys Lett* 375:247
20. Martin BR, Dermody DJ, Reiss BD, Fang M, Lyon LA, Natan MJ, Mallouk TE (1999) *Adv Mater* 11:1021
21. Salem AK, Searson PC, Leong KW (2003) *Nat Mater* 2:668
22. Foss CA, Hornyak GL, Stockert JA, Martin CR (1994) *J Phys Chem* 98:2963
23. Hirata Y, Kyoda H, Hatano H (1994) *Mater Lett* 21:154
24. Prieto AL, Sander MS, Martin-González MS, Gronsky R, Sands T, Stacy AM (2001) *J Am Chem Soc* 123:7160
25. Li X, Zhang X, Li H (2001) *J Appl Polym Sci* 81:3002
26. Masuda H, Fukuda K (1995) *Science* 268:1466
27. Li AP, Müller F, Birner A, Nielsch K, Gösele U (1999) *Adv Mater* 11:483
28. Diaz AF, Castillo JI (1980) *J Chem Soc Chem Commun* 397
29. Kavan L, O'Regan B, Kay A, Grätzel M (1993) *J Electroanal Chem* 346:291
30. Lu Y, Shi G, Li C, Liang Y (1998) *J Appl Polym Sci* 70(11):2169
31. Kim JM, Chang SM, Muramatsu H (1999) *J Electrochem Soc* 146:4544
32. Panero S, Prospero P, Scrosati B (1992) *Electrochim Acta* 37(2):419